ENGINE INTAKE DOWNWASH FOR REAR FUSELAGE MOUNTED NACELLES

R. Slingerland, N.L.S. Moonen

Faculty of Aerospace Engineering
Department of Flight Mechanics and Propulsion
Delft University of Technology
P.O. Box 5058, 2600 GB
Delft, The Netherlands
Phone: +31 15 2785332
E-mail: R.Slingerland@lr.tudelft.nl

Keywords: *downwash, engine intake, horizontal tail*

Abstract

For rear fuselage mounted engines the downwash directly behind the wing is important for several reasons. It determines the variation of angles of attack the intake has to deal with and thus the shape of the intake lip. In addition, it has an impact on the incidence of the nacelle, in order to prevent it from carrying lift in the cruise condition. Finally, as the nacelle will generate lift in other conditions, it has an effect on the downwash the nacelle will produce at the horizontal tail and thus upon stability and control as well as upon trim drag.

Earlier investigations have resulted in a method to determine tail downwash. It is based on analytical expressions in order to facilitate not only rapid application in the preliminary design phase, but accurate application in the detailed design as well. Here a method for incorporating chordwise pressure distribution is presented. Validation by comparison to theory and experimental data of a Fokker 100 showed good agreement of engine intake downwash prediction. The effect of chordwise pressure distribution on tail downwash proved to be very small.

1 Introduction to the method

For tail sizing purposes the tail angle of attack and thus downwash must be estimated as accurately as can be. In recent years much work has been devoted to lifting surface models and computational fluid dynamics (CFD) applications. However, within the preliminary design phase one would rather not turn to CFD tools because of the large amount of numerical models required, each with their own grid, due to design parameter variations.

To the authors knowledge no practical handbook methods are available for the prediction of downwash behind a swept wing with slats and flaps deflected [1]. Thus there is a need for a quick yet accurate estimation of the tail downwash for a swept wing, clean as well as with slats and flaps deflected, suitable for parameter variations so often required during the preliminary design phase.

Therefore a new analytical method has been developed [1]. One important assumption of this method is elliptical lift distribution. Although it seems acceptable, as it is a general design goal for minimum induced drag, one might consider shifting the lift more inboard to reduce wing weight. But for the present purpose it brings a great simplification as it facilitates analytical expressions for the downwash. The method as described in [1] is based on the downwash generated by a lifting line and a trailing vortex sheet. Incorporated in this method are effects of

wing sweep, roll-up and displacement of the vortex sheet as well as the use of high lift devices. It can be applied to configurations with under wing mounted jet engine nacelles as well as rear fuselage mounted engine nacelles. In [2] ground effect was incorporated into this method as it is important for the determination of field performance.

Not only the determination of the downwash at the tail location is important but for rear fuselage mounted engine configurations also the downwash at the engine intake plays a key role for several reasons. For the design of the intake lip the range of angles of attack must be determined. In addition it influences the nacelle incidence, in order to prevent it from carrying lift in the cruise condition. Finally, as the nacelle will generate lift in other conditions it has an effect on the downwash the nacelle will produce at the horizontal tail and thus upon stability and control as well as upon trim drag.
The method as described in [1] and [2] facilitates rapid application in the preliminary design phase as well as accurate application in the detailed design. Although the method relies on today's computer power to solve the set of expressions, it requires very little input.

Application and validation of this method on the downwash at an engine intake of a rear fuselage mounted engine configuration of a modern T-tailed twin jet [1] revealed that the chordwise pressure distribution can not be ignored, as it is usually for tail downwash. Therefore the effect of chordwise pressure distribution is added to this method for clean configurations and configurations with high lift devices deployed. It has not yet been incorporated in the ground effect calculations. Also an effect of wing twist is incorporated in this last version of the method. Not yet incorporated is the effect of wake inflow on downwash.

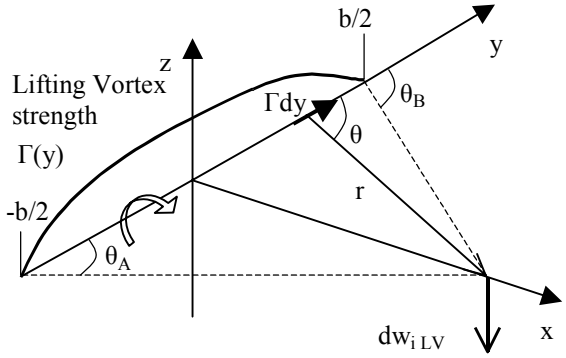

Figure 1: Induced velocity due to lifting vortex

1.2 Influence of chordwise pressure distribution

In the current method Prandtl's lifting line theory is the basis for the description of the lift distribution over the wingspan and the trailing vortex sheet. This lifting line is located at the quarter chord line and the trailing vortex sheet also originates from this line. To concentrate the lifting vortex (and thus the lift) at the quarter chord line instead of spreading it over the chord is a major simplification. From previous results [1] and [2] it is concluded that the lack of modeling chordwise effects of the wing pressure distribution may be the cause of a significant error in the downwash prediction. Therefore a chordwise correction has to be implied. To come to a derivation of this correction a simple lifting line model is analyzed.

The induced velocity field of the wing is now split up in two contributions. The velocity induced by the lifting vortex (LV) and the velocity induced by the trailing vortex sheet (TV). In this simple analysis no vortex sheet displacement, deformations etc. are accounted for. Because we are interested in the downwash at engine intake location and the horizontal tail, a first analysis is made in the aircraft plane of symmetry.

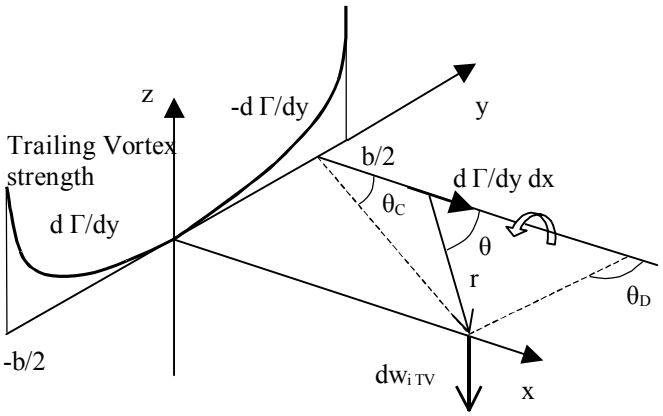

Figure 2: Induced velocity due to trailing vortex

First the contribution of the LV to the induced velocity at the control point in the plane of symmetry is analyzed, see figure 1. The induced velocity due to the lifting vortex can be written as

$$dw_{i\_LV} = -\frac{\Gamma}{4\pi}\frac{\sin(\theta)}{r^2}dy = \frac{\Gamma}{4\pi x}\sin(\theta)d\theta$$
$$w_{i\_LV} = -\frac{\Gamma}{4\pi}\int_{-b/2}^{b/2}\frac{\sin(\theta)}{r^2}dy = \frac{\Gamma}{4\pi x}\int_{\theta_A}^{\theta_B}\sin(\theta)d\theta \qquad (1)$$

From these formulas (1) and from figure 1 it can be concluded that the contribution of the lifting vortex to the induced velocity w_i decreases rapidly with increasing spanwise location from the plane of symmetry, due to decreasing vortex strength and increasing distance r form the vortex element to the control point. Also the influence of chordwise distribution of the lifting vortex strength decreases therefore towards the wing tip. Because the lifting vortex is strongest and of constant strength at the plane of symmetry and directly besides it, it is assumed that only here the influence of a chordwise distribution is worth taking into account. Therefore it is allowed to calculate the effect of the chordwise distribution of the lifting vortex with a two dimensional model.

Now the contribution of the trailing vortex sheet to the induced velocity is analyzed, see figure 2. Again the control point is situated at the plane of symmetry. The strength of the trailing vortices is zero at the plane of symmetry and increases towards a maximum at the tip. The induced velocity can now be written as

$$dw_{i\_TV} = -\frac{1}{4\pi}\frac{d\Gamma}{dy}\frac{\sin(\theta)}{r^2}dx = \frac{1}{4\pi}\frac{d\Gamma}{dy}\frac{\sin(\theta)}{y}d\theta$$
$$w_{i\_TV} = \frac{1}{4\pi}\int_{-b/2}^{b/2}\frac{d\Gamma}{dy}\frac{1}{y}\left\{\lim\int_{\theta_C}^{\theta_{D\to\pi}}\sin(\theta)d\theta\right\}dy \qquad (2)$$

From figure 2 and formulas (2) it can be seen that the influence of chordwise distribution of the TV is much smaller than for the LV. This is mainly due to the fact that the largest TV strength occurs at the wingtip and thus r becomes large. Therefore no chordwise correction will be applied to the downwash caused by the trailing vortex sheet.

1.3 Chordwise correction of lifting vortex induced downwash

From the previous paragraph it is concluded that only the chordwise distribution of the lifting vortex will be taken into account. It was also concluded that the effect of chordwise spreading compared to the concentrated vortex as used can be accounted for by a two dimensional correction.

To calculate these correction factors two models will be compared. A single vortex concentrated at the quarter chord point of a cambered profile and a vortex sheet distributed over the chord with equal strength. The method of modeling and calculation is described in the next section. This section will describe how the calculated induced velocity of the two models is used to create two correction factors that will be used to correct the three dimensional calculation of the downwash induced by the lifting vortex.

For the analysis of the chordwise distribution of the vortex strength a plate with parabolic camber is used. According to thin airfoil theory the vortex distribution is calculated as well as the downwash field around the plate. The integrated vortex strength is then used as the strength of the concentrated vortex, which is located at the quarter chord point. Again the downwash field is calculated.

For the simple parabolic plate vortex distribution, see formulas 3 and 4, an observation can be made; the vortex strength is given by a contribution due to camber A_1 and a contribution depending on angle of attack α. At angle of attack zero only the camber related part remains. For the calculation of the correction factors this division is also made.

$$z(x) = A_1 x(1-x) \tag{3}$$

$$\gamma(x) = 2V_\infty \left(\alpha \sqrt{\frac{1-x}{x}} + 2A_1 \sqrt{x - x^2} \right) \tag{4}$$

The first correction factor is given by the rate of the two dimensional distributed vortex downwash at $\alpha=0$ and the two dimensional downwash of the concentrated vortex

$$k_0 = \left. \frac{\varepsilon_{c\_\alpha=0}}{\varepsilon_{\frac{1}{4}\_\alpha=0}} \right|_{2D} \tag{5}$$

The next factor is given by the ratio of the two dimensional downwash slopes of the distributed vortex strength and the concentrated vortex.

$$k_\alpha = \left. \frac{\left(\varepsilon_c - \varepsilon_{c\_\alpha=0}\right)}{\left(\varepsilon_{\frac{1}{4}} - \varepsilon_{\frac{1}{4}\_\alpha=0}\right)} \right|_{2D} \tag{6}$$

For a given calculation point in the flow field and camber of the airfoil both correction factors can be evaluated to a constant, see figure 3.

The corrected three-dimensional downwash due to the lifting vortex is then calculated according to figure 4 and can be written as

$$\varepsilon_{LV\_3D} = \left(\varepsilon_{\frac{1}{4}\_LV\_3D} - \varepsilon_{\frac{1}{4}\_LV\_3D\_\alpha=0} \right) * k_\alpha + k_0 * \varepsilon_{\frac{1}{4}\_LV\_3D\_\alpha=0} \tag{7}$$

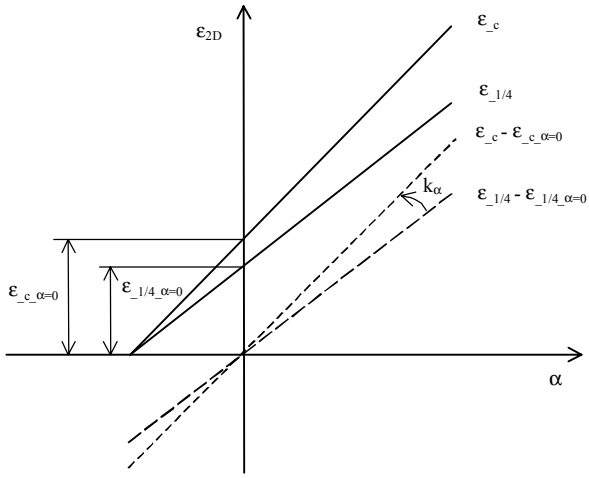

Figure 3: 2-dimensional calculation of k0 and ka

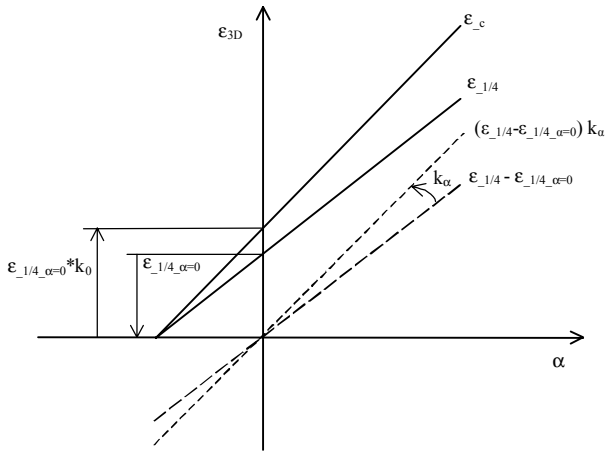

Figure 4: 3-dimensional chordwise downwash correction

2 Modeling the effect of chordwise circulation distribution on downwash angle

2.1 Parabolic plate without flap

As described in the previous section the effect of chordwise circulation distribution instead of the lifting line at the quarter chord line can be taken into account by using a two dimensional correction. This two dimensional correction is obtained by using thin airfoil analysis. A comparison of downwash fields is made for the vortex strength distributed along the chord of the airfoil and a single vortex at the quarter chord point of the airfoil. To represent a thin cambered airfoil it is chosen to use a parabolic plate for a first analysis.

The origin of the reference axis system will be at the leading edge (LE), the x-axis extending along the chord line backwards and the z-axis perpendicular to it, positive upward. The airfoil will be simulated by placing a vortex sheet on the camber line, [3]. To represent the airfoil it is necessary to calculate the vortex strength γ(s) along the camber line in such a way that the camber line becomes a streamline of the flow and such that the Kutta condition is satisfied at the trailing edge (TE), γ(TE)=0. Because the camber line is close to the chord line, the vortex sheet will be placed on the chord line, thus γ= γ(x). The boundary conditions for calculating γ(x) remain the same, i.e. the camber line is a streamline of the flow and the Kutta condition γ(c)=0 is satisfied.

The velocity field is given by the sum of the undisturbed free stream velocity and the induced velocity by the vortex sheet. The slope of the camber line will now be expressed as dz/dx. For the camber line to be a streamline the velocity component perpendicular to the camber line must be zero. After some manipulation this boundary condition can be expressed as

$$\int_0^c \frac{\gamma(\xi)d\xi}{2\pi(x-\xi)} = V_\infty\left[\alpha - \frac{dz}{dx}\right] \tag{8}$$

with a coordinate transformation

$$x = \frac{1}{2}(1-\cos(\theta_0)) \tag{9}$$

formula (1) can be rewritten

$$\frac{1}{2\pi}\int_0^\pi \frac{\gamma(\theta)\sin(\theta)d\theta}{\cos(\theta)-\cos(\theta_0)} = V_\infty\left(\alpha - \frac{dz}{dx}\right) \tag{10}$$

To satisfy the Kutta condition γ(π)=0 a general solution to (10) can be found as

$$\gamma(\theta) = 2V_\infty\left(A_0\frac{1+\cos(\theta)}{\sin\theta} + \sum_{n=1}^{\infty} A_n \sin(n\theta)\right) \tag{11}$$

$$\begin{aligned} A_0 &= \alpha - \frac{1}{\pi}\int_0^\pi \frac{dz}{dx}(\theta)d\theta \\ A_n &= \frac{2}{\pi}\int_0^\pi \frac{dz}{dx}(\theta)\cos(n\theta)d\theta \end{aligned} \tag{12}$$

2.2 Adding a flap to the parabolic plate

To model a flap which extends the chord and deflects, it is convenient to write the formulas in non-dimensionalized form. First a new chord length c_1 is introduced which is expressed as a fraction of the old chord c, depending on flap defection angle δ. New x and z coordinates which are defined as $x=x/c_1$ and $z=z/c_1$ are introduced.

According to [4] the flap is modeled in the same way as the camber of the airfoil. This means that the flap is described as a part of the camber line with constant camber

$$\frac{dz}{dx} = -\tan(\delta) \tag{13}$$

where the boundary condition demands the flow to have this direction.

It has to be pointed out here that the vortex sheet is placed on the extended chord line of the non-flapped airfoil to represent the flap, see figure 5.

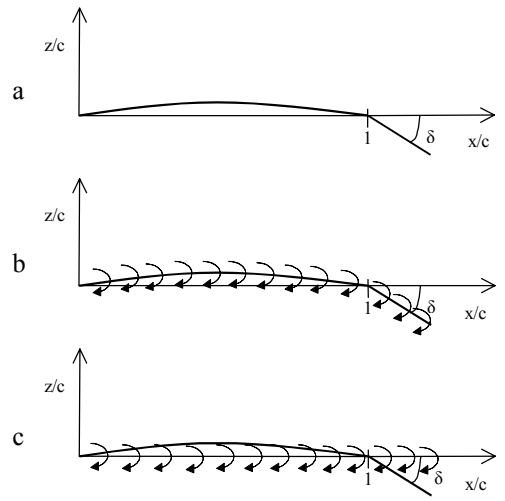

Figure 5: a) parabolic plate with flap

b) vortex sheet

c)simplified vortex sheet

At every point of this vortex sheet, between the flap boundary θ_1 and π the boundary condition (13) is applied. This implies a large simplification in the modeling of flap effect on downwash because the general analytic solution for the vortex strength $\gamma(\theta)$ (11) is still valid. The Fourrier coefficients (12) can then be calculated as

$$A_0 = \alpha - \frac{1}{\pi}\left\{\int_0^{\theta b1}\frac{dz}{dx}(\theta)d\theta - \int_{\theta b1}^{\pi}\tan(\delta)d\theta\right\}$$

$$A_n = \frac{2}{\pi}\left\{\begin{array}{l}\int_0^{\theta b1}\frac{dz}{dx}(\theta)\cos(n\theta)d\theta \\ -\int_{\theta b1}^{\pi}\tan(\delta)\cos(n\theta)d\theta\end{array}\right\} \qquad (14)$$

2.3 Calculation of the flow properties

From the calculations in the previous paragraph the circulation distribution is known. The next step is to calculate the flow properties due to this circulation.

The total circulation equivalent to the distributed vortex strength is defined as the integral over the distributed vortex strength

$$\Gamma = \int_0^{c1}\gamma(x)dx = \frac{1}{2}c_1\int_0^{\pi}\gamma(\theta)\sin(\theta)d\theta \qquad (15)$$

with vortex strength (11) this can be evaluated to

$$\Gamma = c_1 V_\infty\left(\pi A_0 + \frac{\pi}{2}A_1\right) \qquad (16)$$

The section lift coefficient is then by definition

$$c_l = \frac{\rho V_\infty \Gamma}{\frac{1}{2}\rho V_\infty^2 c_1} = \pi(2A_0 + A_1) \qquad (17)$$

with substitution of (14) into (17) it follows that

$$c_l = 2\pi\left(\alpha + \frac{1}{\pi}\left\{\begin{array}{l}\int_0^{\theta b1}\frac{dz}{dx}(\theta)(\cos(\theta)-1)d\theta \\ -\int_{\theta b1}^{\pi}\tan(\delta)(\cos(\theta)-1)d\theta\end{array}\right\}\right)$$

$$c_{l_\alpha} = 2\pi \qquad (18)$$

$$\alpha_0 = -\frac{1}{\pi}\left\{\begin{array}{l}\int_0^{\theta b1}\frac{dz}{dx}(\theta)(\cos(\theta)-1)d\theta \\ -\int_{\theta b1}^{\pi}\tan(\delta)(\cos(\theta)-1)d\theta\end{array}\right\}$$

2.4 Calculation of the induced velocities

The induced velocity in a calculation point $p=(x_p; z_p)$ by a vortex filament of strength γ and length ds can be expressed as

$$dV_i = -\frac{\gamma ds}{2\pi r} \qquad (19)$$

where r is the distance from the vortex element to the calculation point and dV acts perpendicular to this radius.

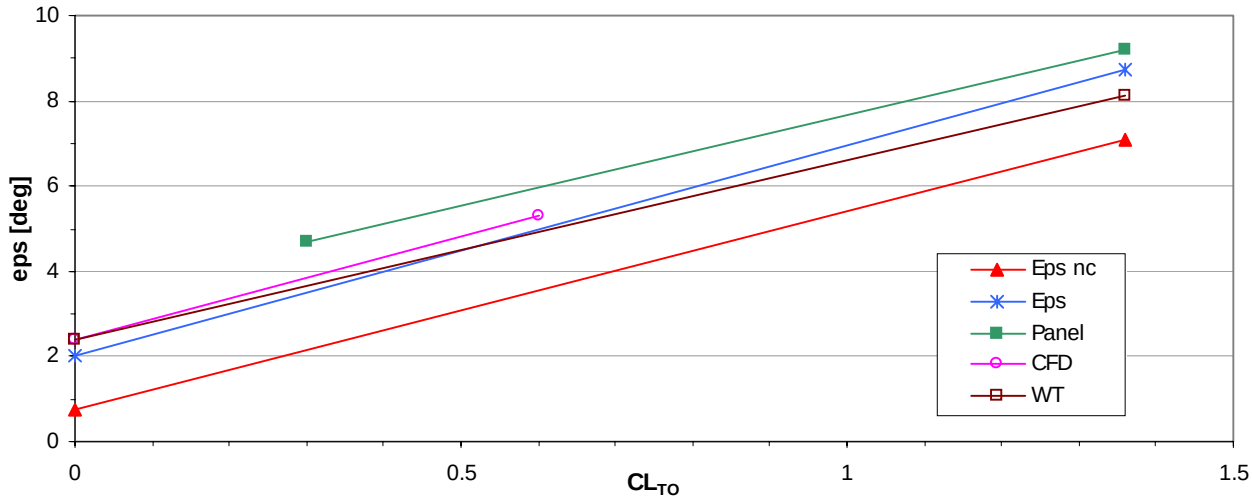

Figure 6: Fokker 100 engine intake downwash, clean configuration

To be able to determine the total integrated induced velocity in p it is necessary to decompose the contributions of each vortex element into fixed directions, the x and z direction of the chord axis system. For a vortex element located on the chord at a distance s from the LE the two velocity components are

$$dV_{i\_x} = \frac{\gamma}{2\pi} \frac{z_p}{(x_p - s)^2 \left(1 + \frac{z_p^2}{(x_p - s)^2}\right)} ds$$
$$dV_{i\_z} = -\frac{\gamma}{2\pi} \frac{1}{(x_p - s) \left(1 + \frac{z_p^2}{(x_p - s)^2}\right)} ds \qquad (20)$$

For this calculation γ from (11) was first transformed back to chordwise x coordinates with (9).

To obtain the induced velocities in the axis system of the undisturbed flow a rotation has to be performed

$$dV_{i\_x\_\infty} = dV_{i\_x}\cos(\alpha) + dV_{i\_z}\sin(\alpha)$$
$$dV_{i\_z\_\infty} = dV_{i\_z}\cos(\alpha) - dV_{i\_x}\sin(\alpha) \qquad (21)$$

and by integration over the total chord c_1

$$dV_{i\_x\_\infty} = \int_0^1 dV_{i\_x\_\infty} ds$$
$$dV_{i\_z\_\infty} = \int_0^1 dV_{i\_z\_\infty} ds \qquad (22)$$

The total velocities in the calculation point p

$$V_{p\_x\_\infty} = V_\infty + V_{i\_x\_\infty}$$
$$V_{p\_z\_\infty} = V_{i\_z\_\infty} \qquad (23)$$

The downwash angle is then by definition

$$\varepsilon = \arctan\left(\frac{-V_{i\_z\_\infty}}{V_\infty + V_{i\_x\_\infty}}\right) \approx -\frac{V_{i\_z\_\infty}}{V_\infty} \qquad (24)$$

It was found that the rotation to the undisturbed stream axis system is not significant for the result in downwash, therefore the downwash will be calculated as

$$\varepsilon = -\frac{V_{i\_z}}{V_\infty} \qquad (25)$$

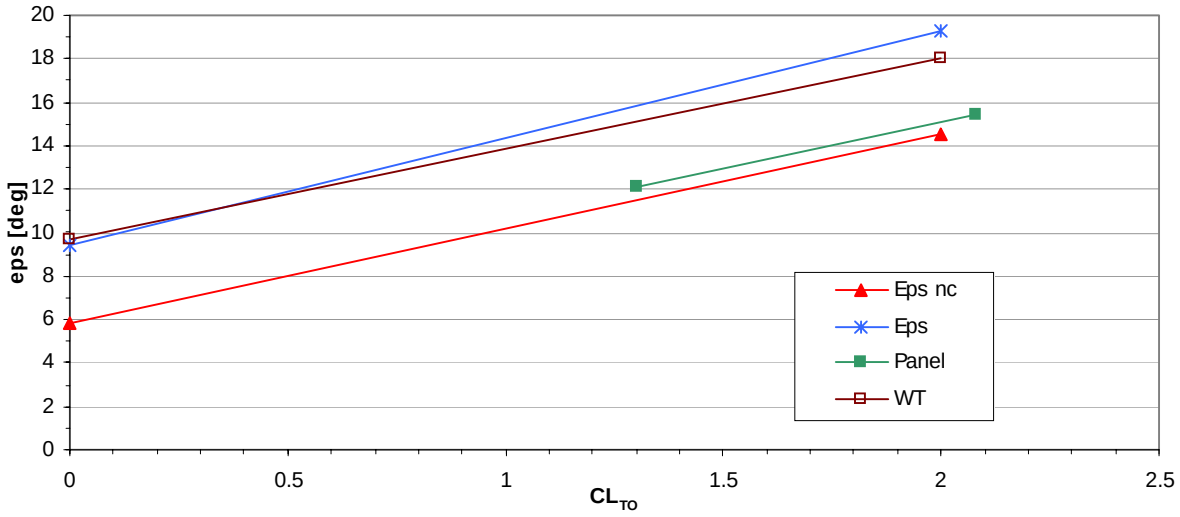

Figure 7: Fokker 100 intake downwash, landing flaps

3 Results

3.1 Calculation and reference methods

To evaluate the effect of the additional correction for chordwise lift distribution calculations were made for the Fokker 100. This is a T-tailed aircraft with engines mounted on the aft fuselage. The calculations were made with the downwash calculation procedure as described in [1] with and without the chordwise correction. This method will be called "eps" in the figures. It has to be pointed out that the effect of nacelle lift on tail downwash is not yet incorporated in this method and was calculated separately. The conditions without chordwise correction will be referred to as "nc". All downwash data are plotted against CL tail-off (CL_{TO}).

The effect of nacelle lift on tail downwash was calculated with a method called "HOT" which is a horizontal tail sizing program. Actually eps is a smaller version of HOT only to calculate downwash without nacelles. HOT has the option of calculating downwash with and without the effect of nacelles. The chordwise correction module from eps was not yet incorporated in HOT. Therefore HOT is only used to show the effect of nacelle lift on tail downwash without chordwise correction by calculation of tail downwash with and without nacelles ("no nac"). Then the effect of different engine intake downwash due to chordwise correction was manually calculated from the engine intake downwash calculated with eps and the nacelle effect of HOT.

Further reference data for the intake downwash are a panel code calculation which is referred to as "panel", a CFD calculation referred to as "CFD" and wind tunnel test derived data referred to as "WT". It should be kept in mind that these reference data were not dedicated downwash calculations and measurements. Downwash was derived from it using aerodynamic coefficients from ESDU methods. This reduces the reliability of these data.

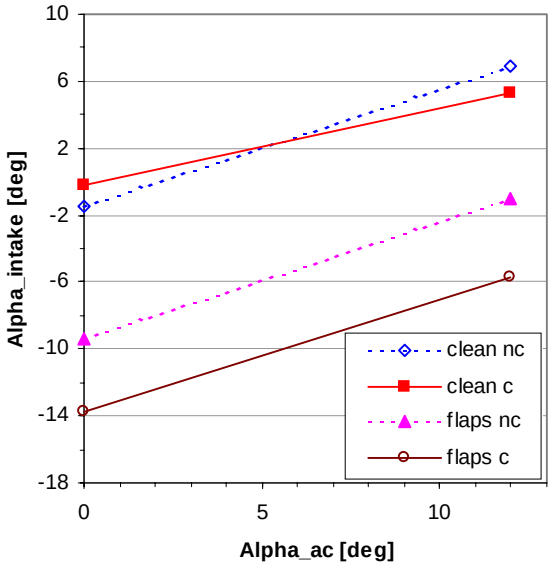

Figure 8: Engine intake downwash Fokker 100

3.2 Intake downwash clean configuration

The results of the calculations with eps and eps_nc for the engine intake downwash for the Fokker 100 in clean configuration are shown in figure 6. It is seen that eps_nc underestimates the intake downwash for zero lift ε_0 by 1.5 to 2.5 degrees. The slope $d\varepsilon/d\alpha$ lies within the scatter of the reference data. When the chordwise correction is applied method eps delivers very good results for the intake downwash. The ε_0 is predicted within 0.3 degrees relative to the CFD calculations and WT derived data. The gradient $d\varepsilon/d\alpha$ of eps is a perfect match with the CFD data but a little bit larger than the panel and the WT gradient. Over the whole range the prediction of eps is within a half degree relative to the WT data series. Therefore it may be concluded that the chordwise correction provides a large improvement of the intake downwash in clean configuration. A good match with reference data is the result.

3.3 Intake downwash landing flaps

The results of the calculations with eps and eps_nc for the engine intake downwash for the Fokker 100 with flaps extended in the landing position are shown in figure 7. It is seen that although eps_nc underestimates the intake downwash over the whole range, the slope is predicted well without chord correction. The chord correction is larger with flaps extended than clean as expected. Prediction of ε_0 is very close to WT data although slope $d\varepsilon/d\alpha$ is a little bit higher than both WT and panel data. However over the whole range of lift coefficient a good prediction of intake downwash with flaps extended was found with eps including the chord correction. Relative to the WT data the prediction is within one degree over the whole operating range.

It may be concluded that the method eps including the chordwise correction provides an accurate prediction of intake downwash for a clean configuration as well as for a configuration with flaps extended. In both cases the prediction was very close to the WT data set over the whole operating range of lift coefficient.

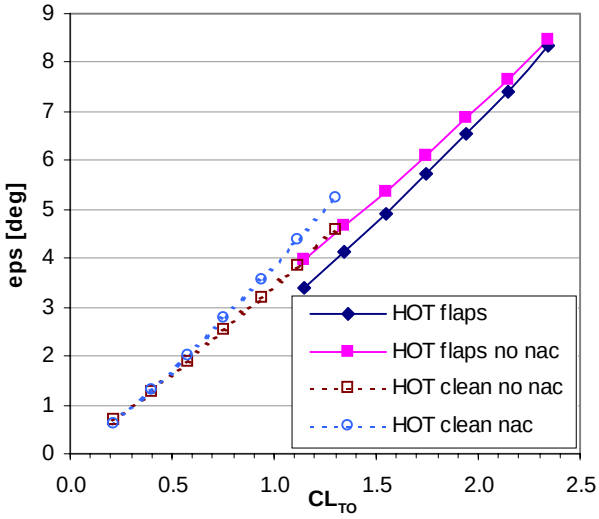

Figure 9: Horizontal tail downwash Fokker 100, clean and landing flaps

3.5 Tail downwash

3.5.1 Tail downwash contributions

Tail downwash is mainly generated by two contributions: first the direct downwash from the wing and the flaps and their vortex systems, second the downwash generated by a lift-carrying nacelle. The direct effect of chordwise correction on tail downwash is small and almost constant (approximately +0.2º clean and +0.5º with landing flaps) because of the relatively large distance from wing to tail.

The second effect of chordwise correction is a change in engine intake downwash and therefore a change in intake angle of attack α_{int}. This changes the lift over the nacelle and therefore the tail downwash generated by the nacelle lift.

In figure 8 α_{int} is shown as function of airplane angle of attack α_{ac} for a clean and landing flap configuration with and without chordwise correction. For the clean configuration it is seen that α_{int} is larger at $\alpha_{ac}=0^\circ$ but that it has a smaller slope so that at $\alpha_{ac}=12^\circ$ α_{int} with chord correction is smaller than without.

3.5.2 Clean configuration

For $\alpha_{ac} > 2^\circ$, $\alpha_{int\_no\ chord} > 0^\circ$ and thus the nacelle is carrying lift and gives a positive contribution to the tail downwash as can be seen from figure 9 where tail downwash without chordwise correction is calculated with and without nacelle effect. Due to the change in α_{int} when the chordwise correction is applied to the intake downwash this additional tail downwash will be smaller for $\alpha_{ac} > 5^\circ$ and larger for smaller α_{ac}. This is the crossover point in figure 8 where $\alpha_{int\_chord} = \alpha_{int\_no\ chord}$.

Relative to HOT without nacelles from figure 9 a positive contribution of nacelle lift to tail downwash in clean configuration starts at $\alpha_{ac}=0.5^\circ$ and rises to an increase of 0.7° $\alpha_{ac}=12^\circ$. This effect is small, even together with the direct chord effect of $+0.2^\circ$ a total contribution to tail downwash at $\alpha_{ac}=12^\circ$ of approximately 1° is found.

3.5.2 Landing flaps configuration

With flaps deflected (no chord correction) tail downwash decreases due to negative nacelle lift as can be seen in figure 9. Due to chordwise correction of the downwash at the engine intake α_{int} becomes more negative see figure 8, which results in a larger negative correction of HOT w/o nacelles (-0.9° at $\alpha_{ac}=0^\circ$, -1.1° at $\alpha_{ac}=12^\circ$). Together with the direct chordwise correction of tail downwash of $+0.5^\circ$ an almost constant effect of -0.5° relative to HOT w/o nacelles remains for total nacelle and chordwise correction.

It is observed that the direct chordwise correction of tail downwash and the effect of chordwise correction of intake downwash on tail downwash cancel each other in the case of flaps extended.

4 Conclusions

The effect of chordwise pressure distribution has a significant effect on engine intake downwash and angle of attack for rear fuselage mounted engines. The modeling of these chordwise effects into method eps provided an improvement to the method. This method now is capable of an accurate prediction of engine intake downwash for rear fuselage mounted engine nacelles as was evaluated by using it for a Fokker 100. The method provides good results for clean configuration as well as the landing flap configuration.

The effect of chordwise pressure distribution on tail downwash which was suspected to contribute to an error in ε_0 as described in [1] and [2] proved to be small. For the clean configuration a net chord effect remains, for the landing flap configuration the direct chord effect and the change in nacelle generated downwash cancel each other. However the effect of nacelle generated downwash remains significant.

References

[1] García E, Nispen van A and Slingerland R. Downwash at the tail of swept-wing transports with high-lift devices, *AIAA 2001-5237*, 2001.

[2] Slingerland R. Tail downwash in ground effect of swept-wing jet transports with high-lift devices. *CEAS Aerospace Aerodynamics Research Conference*, Cambridge, 2002.

[3] Anderson J.D. *Fundamentals of aerodynamics*. 2nd edition, McGraw-Hill, 1991.

[4] Moonen N.L.S. *Bepaling van de geïnduceerde snelheden rond een vleugelprofiel met klep m.b.v. potentiaaltheorie voor dunne profielen*. Delft University of Technology, 2001.